Revista Iberoamericana para la Investigación y el Desarrollo Educativo
ISSN 2007 - 7467

https://doi.org/10.23913/ride.v16i32.2959

Scientific articles

Calibración de impresora 3D cerámica: teórico-práctico

Calibration of ceramic 3D printer: theoretical–practical

Calibração de uma impressora 3D de cerâmica: teoria e prática

Juan José Avila Navarrete
Universidad de Guadalajara, México
juan.anavarrete@alumnos.udg.mx
https://orcid.org/0009-0000-9141-4265

José Antonio Muñoz-Gómez*
Universidad de Guadalajara, México
antonio.munoz@academicos.udg.mx
https://orcid.org/0000-0002-8724-8302

Abimael Jiménez Pérez
Universidad Autónoma de Ciudad Juárez, México
abimael.jimenez@uacj.mx
https://orcid.org/0000-0002-9514-4570

Omar Aguilar Loreto
Universidad de Guadalajara, México
omar.aguilar@academicos.udg.mx
https://orcid.org/0000-0002-0395-0066

Resumen

La tecnología de impresión 3D y la integración de materiales cerámicos con la técnica de extrusión directa es un método moderno que permite imprimir formas complejas con materiales viscoelásticos. En este trabajo se presenta un estudio de calibración, tanto teórico como experimental, aplicado a una impresora 3D de bajo costo. El material de impresión es una pasta cerámica compuesta principalmente de base acrílica Ready-Mix y cemento blanco. Primero, se evaluaron nueve combinaciones de velocidad de impresión en el rango de 10 mm/s a 20 mm/s, y una velocidad de extrusión en el rango de 20 mm/s a 25 mm/s, mediante

un análisis empírico, con el objetivo de identificar rangos de operación estable. Posteriormente, se desarrolló un modelo matemático del sistema de extrusión para determinar teóricamente los parámetros óptimos de las velocidades de extrusión y desplazamiento (v_e=22.09 mm/s, v_{xy}=17.08 mm/s). La validación experimental determinó que los parámetros obtenidos con el modelo matemático permiten una deposición continua, estable y con mayor precisión geométrica en comparación con el ajuste empírico.

Palabras clave: extrusión directa, impresión 3D, modelo matemático, pasta cerámica.

Abstract

3D printing technology and the integration of ceramic materials with the direct extrusion technique represent a contemporary method that enables complex shapes to be printed with viscoelastic materials. In this paper, we present a calibration study, both theoretical and experimental, applied to a low-cost 3D printer. The printing material is a ceramic paste primarily composed of a Ready-Mix acrylic base and white cement. Initially, nine combinations of print speed in the range of 10 mm/s to 20 mm/s, and extrusion speed in the range of 20 mm/s to 25 mm/s, were evaluated through empirical analysis, with the aim of identifying stable operating ranges. Subsequently, a mathematical model of the extrusion system was developed to theoretically determine the optimal parameters of extrusion and displacement speeds (v_e = 22.09 mm/s, v_{xy} = 17.08 mm/s). The experimental validation determined that the parameters obtained with the mathematical model allow a continuous, stable deposition with enhanced geometric precision compared to the empirical fit.

Keywords: direct extrusion, 3D printer, mathematical model, ceramic paste.

Resumo

A tecnologia de impressão 3D e a integração de materiais cerâmicos com a técnica de extrusão direta representam um método moderno que permite a impressão de formas complexas com materiais viscoelásticos. Este trabalho apresenta um estudo de calibração, tanto teórica quanto experimental, aplicado a uma impressora 3D de baixo custo. O material de impressão é uma pasta cerâmica composta principalmente de base acrílica Ready-Mix e cimento branco. Inicialmente, nove combinações de velocidade de impressão, na faixa de 10 mm/s a 20 mm/s, e velocidade de extrusão, na faixa de 20 mm/s a 25 mm/s, foram avaliadas

empiricamente para identificar faixas de operação estáveis. Posteriormente, um modelo matemático do sistema de extrusão foi desenvolvido para determinar teoricamente os parâmetros ótimos para as velocidades de extrusão e deslocamento (v_e = 22,09 mm/s, v_xy = 17,08 mm/s). A validação experimental determinou que os parâmetros obtidos com o modelo matemático permitem uma deposição contínua e estável com maior precisão geométrica em comparação ao ajuste empírico.

Palavras-chave: extrusão direta, impressão 3D, modelo matemático, pasta cerâmica.

Date Received: September 2025 **Date Accepted:** May 2026

Introduction

In recent decades, 3D printing technology has had a considerable impact on various scientific and engineering sectors, including the manufacture of mechanical components, athletic footwear, medical prostheses, lightweight structures, functional prototypes, and, more recently, the *on-site 3D printing* of residential structures (Bose et al., 2024; Conner et al., 2014; Gibson et al., 2015; Yousaf et al., 2024; Zaborovskii et al., 2025). This novel paradigm represents a transformation in small-scale manufacturing processes, establishing itself as a promising technology in the medical field and in the development of new materials (H. Chen et al., 2022; Feng et al., 2019; Ngo et al., 2018; Yan et al., 2018). Its primary attributes include the ability to efficiently manufacture complex structures, customize them, and progressively reduce costs.

Ceramic materials exhibit diverse properties, such as high hardness, thermal resistance, low electrical conductivity, chemical stability, and corrosion resistance (Carter and Norton, 2013; Somiya, 2013). These characteristics make them relevant in high-tech industries, such as energy, aerospace, military, and chemical (Ford and Despeisse, 2016). The integration of ceramic materials into 3D printing presents an opportunity to expand their fields of application.

3D printing of ceramics is a cutting-edge technology that overcomes the limitations of traditional ceramic molding. It offers several significant advantages, including reduced mold-making costs, simplified processes, and the possibility of automated operation (Lewis and Gratson , 2004; Romanczuk-Ruszuk et al., 2023). Various technologies are available for printing ceramic materials, including direct ink extrusion. Digital Image Writing (DIW) stands out for providing a pioneering technological approach to printing ceramic materials

with moderate to low viscosities. In this technique, the material is deposited layer by layer, accurately replicating the three-dimensional shape of the digital object.

The material is deposited using an extruder, in which a helical screw applies pressure to the viscous paste, allowing precise control of the amount of material deposited by regulating the extrusion speed. This technology is characterized by its ability to extrude viscoelastic materials, such as ceramic pastes, without the need for a thermal fusion process (Lewis, 2006). This offers significant advantages, including the possibility of incorporating functional additives, reduced energy consumption and waste, and compatibility with a wide range of natural materials (Tagliaferri et al., 2021).

Fused deposition modeling (FDM) printers have been adapted for printing ceramic materials. By modifying the mechanical structure and extrusion head, a commercial ceramic clay from the WASP brand, prepared with a water/clay ratio in the range of 0.57 to 0.69, was successfully processed. Experimental results validated the ability to print complex geometries, achieving a compressive strength of up to 9.6 MPa after drying and firing (Chaari et al., 2022).

Alonso Madrid et al. investigated the reuse of commercial clays using two commercial printers. Through an experimental study, they demonstrated that the printing-recycling cycle can be carried out indefinitely, provided that the incorporation of cementitious materials or additives is avoided. Additionally, they validated the feasibility of printing pieces with dimensions up to 25 cm; however, for larger pieces, it is necessary to incorporate additives that improve the mechanical properties of the pieces (Alonso Madrid et al., 2023).

In the study conducted by Diegel et al. (2012), a porous ceramic material was developed by modifying a low-cost 3D printer for the purpose of printing composite materials. The results obtained validated the feasibility of the proposal, demonstrating that the production of porous ceramic filters can be controlled by varying parameters such as printing saturation, material composition, and firing time.

In 2021, Hu et al. developed a theoretical framework for the DIW printing process. They proposed an in-situ shape retention strategy using hot air coupled to the nozzle. Theoretically, they derived a flow balance equation that establishes a relationship between layer height, extrusion speed, and travel speed. This equation is useful for defining optimal operating windows that enhance interlayer adhesion and minimize irregular filament morphologies (Hu et al., 2021).

In 2023, Lin et al. conducted research on the 3D printing process of ceramics, focusing on the analysis of the most relevant printing parameters. This theoretical-practical study concluded that extrusion speed is the critical parameter for achieving optimal quality in printed objects. The research reveals an inherent limitation in the current market: the absence of fully automated ceramic 3D printers capable of self-regulating flow and printing speeds. Consequently, further research is required to comprehend the interaction of viscous flow within a 3D printing machine (Lin et al., 2023).

This paper analyzes the calibration process of a direct extrusion ceramic 3D printer. The study is developed from two complementary approaches: experimental and theoretical. To this end, the morphological effect of varying the extrusion speed (v_e) and the printing speed (v_{xy}) on the printing process of a regular geometric object was evaluated. Based on an experimental design, the ranges of values $v_e = \{10,15,20\}$ mm/s and $v_{xy} = \{20,22.5,25\}$ mm/s were studied. Subsequently, a mathematical model was formulated that incorporates the extrusion process with the screw conveyor, enabling the theoretical determination of the extrusion and displacement parameters.

The study demonstrates that, while the empirical method achieves functional results with adequate layer adhesion, applying the mathematical model guarantees a more stable 3D print with higher geometric resolution. This preliminary work contributes to the characterization of a 3D printer and to the understanding of the dynamic behavior of ceramic paste.

Methodology

The printing system was calibrated by analyzing two critical parameters: extrusion speed (v_e) and printing speed (v_{xy}). These parameters directly influence filament stability, surface quality, and dimensional accuracy of the printed parts.

The calibration procedure was approached using two distinct methods: empirical and theoretical. The empirical method consists of performing 3D printing tests by varying the values of v_{xy} and v_e within a defined range. The theoretical method focuses on estimating the parameters using a mathematical model that considers the extruder's geometry. In both phases, a 25 mm × 25 mm × 25 mm cube, printed with 1 mm layers, was used as a print pattern, allowing for systematic evaluation under controlled conditions. The following sections provide detailed descriptions of the calibration process.

3D ceramic printer

Figure 1 depicts the Tronxy Moore-1 3D printer, selected for its low cost (approximately $500 USD) and educational value. This device fosters innovation and serves as an initial research tool for public educational institutions.

Figure 1: 3D printer for ceramic pastes.

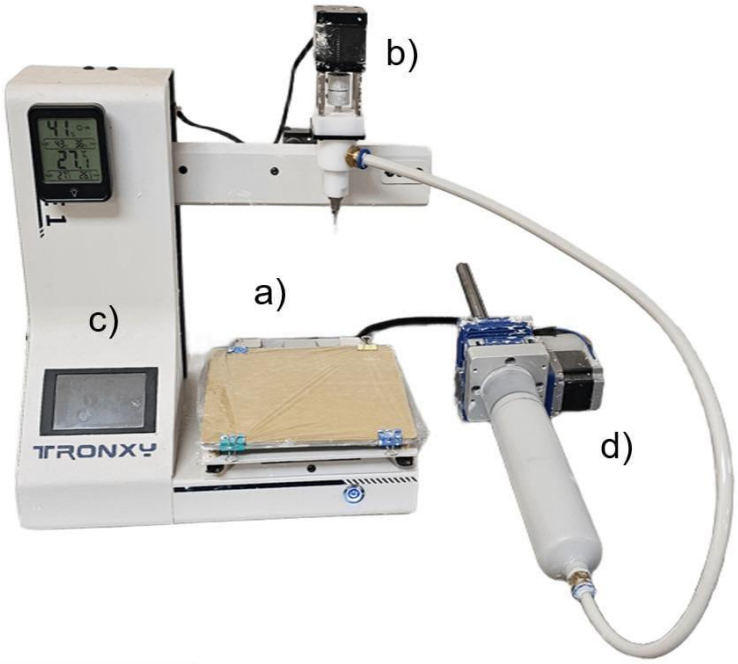

Source: own elaboration.

The main components of the printer include: (a) a movable table that moves along the Cartesian *x - y coordinates* , onto which the material is deposited layer by layer during the manufacturing process; (b) an extruder, responsible for the final extrusion step to precisely deposit the material; (c) an interactive control interface that allows for configuring and monitoring printing parameters; and (d) a loading cartridge, where the printing material is stored. The primary propulsion of the ceramic paste is achieved by an auger located inside the cartridge, which continuously supplies the flow of the ceramic paste to the printer.

Empirical model

In an experimental study, the printing of a cubic solid was evaluated by varying the printing speed (10, 15 and 20 mm/s) and the extrusion speed (20, 22.5 and 25 mm/s). Nine

experimental combinations were obtained, as shown in Table 1. The selected range was defined based on the experience acquired in developed 3D printing processes.

Table 1 . Analysis parameters in the empirical model.

Print speed v_{xy}(mm/s)	Extrusion speedv_e (mm/s)		
10	20	22.5	25
15	20	22.5	25
20	20	22.5	25

Source: own elaboration.

The remaining printing parameters were assigned using Ultimaker Cura slicing software version 5.0. The settings included a layer height of 1 mm and a nozzle size of 1.5 mm. The infill pattern, line width, and absence of retraction were also kept constant. Testing was conducted under controlled environmental conditions, with an average temperature of 29 ± 2 °C and relative humidity ranging from 60–70%.

The ceramic paste used was developed from a recent study (Avila et al., 2025). In this study, a commercial acrylic base (Ready-Mix) was modified by incorporating kaolin (20%), cement (10%), and borax (0.5%). The cited study demonstrated that this composition offers adequate mechanical strength and extrudability, resulting in a paste suitable for 3D printing.

Each print was evaluated using a quantitative and qualitative process. The quantitative evaluation involved measuring the three-dimensional geometry of the printed cube using a digital caliper, thus determining the dimensional error along each coordinate axis. The qualitative evaluation consisted of the following aspects: (a) overextrusion, characterized by excessive material buildup; (b) underextrusion, identifiable by thin filaments, interlayer voids, poor layer adhesion, and structural collapse; and (c) edge distortion and loss of geometric definition. These indicators facilitated the evaluation of print quality in both the experimental and theoretical models.

Mathematical model

This section presents the mathematical model of the 3D printer's extrusion system, which allows for the estimation of the printing's operational parameters. The derivation presented is based on the work of Hu et al. (2021), whose primary contribution lies in a detailed analysis that elucidates the construction of the mathematical model in a clear and concise manner.

Based on the principle of conservation of mass in a steady state, the model determines the geometric and kinematic configuration of the system, thereby facilitating a deeper understanding of the kinematic flow during the ceramic paste deposition process.

It is assumed that the volume displaced—of the ceramic paste—by the screw conveyor is equivalent to the volume that passes through the nozzle and, consequently, to the volume deposited on the impression plate, layer by layer. This conservation principle is expressed as:

$$V_{\text{husillo}} = V_{\text{extruido}} = V_{\text{externo}} \quad (1)$$

where V_{husillo} represents the volume displaced in the screw, V_{extruido} the volume of output through the nozzle, and V_{externo} the volume deposited in the printed path. The extrusion speed, v_e(mm/s), is determined by analyzing the geometric parts, in millimeters, that constitute an extrusion screw, as shown in Figure 2.

Figure 2. Geometric parameters of the screw.

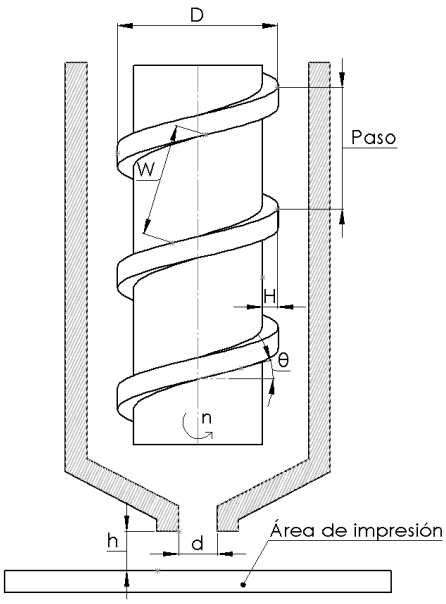

Source: Own elaboration.

The device exhibits uniform circular motion, such that the rotational speed n in rpm can be defined as the number of revolutions the spindle makes per unit of time. The tangential linear speed v of the screw is determined by multiplying the angular speed by the circumference πD, where D represents the screw's outer diameter. The corresponding mathematical relationship is $v = n\pi D$.

The magnitude of the tangential velocity partially displaces the mass within the screw channel, implying the displacement of only a component projected along the direction parallel to the thread's inclination. Consequently, an effective tangential velocity can be calculated $v_{efectiva}$, expressed by the formula $v_{efectiva} = n\pi D cos\theta$.

According to the principle of conservation of angular momentum, the magnitudes of the linear momentum vectors tangential to the plane of rotation and radial from the axis of rotation are inversely proportional. Consequently, the mass rotates at different speeds depending on the tooth height *H*. This relationship allows us to approximate the average effective tangential speed as $\langle v_{efectiva} \rangle = \frac{1}{2} n\pi D cos\theta$ without compromising the model's accuracy.

Finally, the amount of material displaced in the cross-section of the screw channel is denoted as $\langle v_{efectiva} \rangle$. This cross-section, considered the area of interest, is calculated as WH, where W is the width of the screw channel and H is the tooth height. By combining $\langle v_{efectiva} \rangle$ and WH is obtained the expression for the so-called drag flow Q_d along the spindle:

$$Q_d = \frac{1}{2} \pi WHD\, n cos\, \theta \tag{2}$$

Using Equation (2), it is possible to determine the volume of material displaced inside the screw $V_{husillo}$ of Equation (1). This volume is obtained by multiplying Q_d by the time:

$$V_{husillo} = Q_d t. \tag{3}$$

Furthermore, by analyzing the extruder nozzle, it is possible to determine the volume of material that emerges. This corresponds to the term $V_{extruido}$ from Equation (1) and is calculated considering the volume of a small cylinder of radius $d/2$ where d corresponds to the nozzle diameter. The volume is equal to the product of the cylinder's cross-section $\frac{\pi d^2}{4}$ and the height $v_e t$, where v_e represents the extrusion speed. In this way, it obtains:

$$V_{extruido} = \frac{\pi d^2}{4} v_e t. \tag{4}$$

Comparing Equations (3) and (4) and applying the principle of conservation of mass in the process, we can assume that $V_{extruido} = V_{husillo}$, which allows us to calculate v_e as:

$$v_e = \frac{2WHD\cos\theta}{d^2}n, \quad (5)$$

where θ is the fillet angle in radians.

To determine the volume of material deposited beyond the nozzle, the external material volume is essential. This can be calculated by considering the 3D printing speed, which primarily depends on the xy extruder's movement in the plane and the amount of material deposited by the nozzle. This approach assumes that the deposited material corresponds to a surface cross-section composed of two geometric contributions.

The first contribution corresponds to the area of a rectangle with a base d (equal to the diameter of the nozzle) and a height h (equal to the distance between the nozzle and the printing surface). The second contribution represents the excess material at the edges, modeled as a semicircle at each end, equivalent to a full circle of diameter h. The thickness of the deposited material is considered to be approximately equal to the height h. Therefore, the volume of external material is obtained as the sum of both contributions:

$$V_{externo} = v_{xy}t\left(hd + \frac{\pi h^2}{4}\right). \quad (5)$$

Applying the principle of conservation of mass again, by equating $V_{externo} = V_{extruido}$, the following expression is obtained for the displacement speed of the extruder in the *xy plane* .

$$v_{xy} = \frac{\pi d^2 v_e}{4hd+\pi h^2} \quad (6)$$

This analysis enables for explicit determination of the values of v_e y v_{xy}. Through geometric measurements of the extruder, the necessary parameters are obtained to estimate v_e and v_{xy}. These are then incorporated into the 3D printer's slicing software. In this way, it is possible to manufacture ceramic parts considering the geometric characteristics of the worm gear.

Results

This section presents the results of the empirical fitting and the mathematical model applied to the direct extrusion printing process of the ceramic paste. Initially, the combination of printing speed (v_{xy}) and extrusion speed (v_e) was investigated to identify a working window that ensures continuous deposition, good interlayer adhesion, and a stable geometry. Subsequently, a mathematical model of the screw conveyor was used to estimate the values

of v_{xy} and v_e. Using both approaches, nine printing tests were performed on a cubic geometry for results analysis.

Experimental setting

In this study, nine combinations resulting from varying three printing speeds (10, 15, 20 mm/s) and three extrusion speeds (20, 22.5, 25 mm/s) were evaluated. Table 2 summarizes the experimental conditions and the predominant morphological effect observed in each case. Through a visual inspection process, the morphological forms associated with overextrusion (layer buildup, filament widening, convex edges, loss of geometric definition), underextrusion (thickened filaments, interlayer discontinuities, internal voids, final height less than nominal), and structural collapse due to plastic deformation accumulation were evaluated.

Table 2. Conditions evaluated and morphological observations.

Print speed v_{xy}(mm/s)	**Extrusion speedv_e (mm/s)**	**Observations**
10	20	Thin filaments; loosely adhered layers
10	22.5	Overextrusion; partial collapse
10	25	Overextrusion; total collapse
15	20	Accumulation in corners; deformed filaments
15	22.5	Subextrusion; non-homogeneous filaments
15	25	Overextrusion; pronounced lateral deformation
20	20	Subextrusion; poor adhesion
20	22.5	Adequate stability; good resolution
20	25	Acceptable geometry; lower resolution compared to v_e22.5 mm/s

Source: own elaboration.

As can be seen in the lower portion of Table 2, the combination of a travel speed of 20 mm/s with a printing speed of 22.5 mm/s generates the best geometric quality.

The aforementioned behaviors align with the window-based approach to operation. For instance, Chen et al. focus on conducting tests that assess the the mixture's extrudability over time, its ability to maintain its geometry under its weight, and propose its evaluation through both online and offline tests. The experimental tests explain the high flow rate/velocity and the origin of the layer thickening with convex edges. In contrast, at low flow rates, thinned layers with interlayer voids are generated (Y. Chen et al., 2021).

Figure 3 presents the three most representative specimens of the study, accompanied by their geometric reference: (a) 3D computational model of the cube, (b) overextrusion (v_{xy}=15 mm/s, $v_e = 25$ mm/s), (c) filament broadening and non-uniform stacking (v_{xy}=15 mm/s, $v_e = 20$ mm/s), and (d) the most stable condition achieved experimentally (v_{xy}=20 mm/s, $v_e = 22.5$ mm/s). The latter is characterized by continuous deposition, satisfactory adhesion, and the absence of structural deformations in the upper layers.

Figure 3. Comparison of prints under specific printing speed and extrusion conditions.

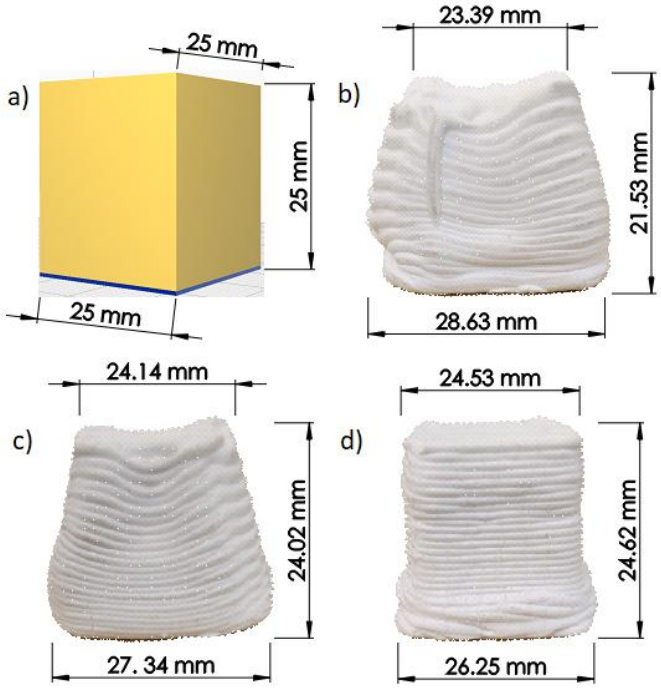

Source: own elaboration.

Through the experimental process, the optimal option was identified within a search range by varying v_{xy} y v_e. However, the dimensional accuracy required for high-precision, high-quality additive manufacturing standards was not achieved, highlighting the inherent limitations of empirical adjustment and suggesting the need to transition towards quantitative calibration using a mathematical model that optimizes the parameters.

Theoretical adjustment

The parameters of the extruder's mathematical model were measured with a high-precision digital vernier caliper (± 0.002 mm), resulting in the following values: screw outer diameter (D) of 14 mm, channel width (W) of 5.33 mm, tooth height (H) of 3.32 mm, a thread angle of 0.785 rad , and a rotation speed of 0.3 rpm. Using these values in equation (4) yields

$$v_e = 22.09\, mm/s \tag{7}$$

Considering a layer height of 1.0 mm and a nozzle diameter of 1.5 mm, using equation (6) a horizontal displacement speed of

$$v_{xy} = 17.08\, mm/s \tag{8}$$

Applying these values, the test geometric cube was printed, resulting in a continuous and consistent deposition (as depicted in Figure 4). The printing time was 17 minutes. Regular layers were observed, without interruptions or excessive material accumulation, indicating a suitable equilibrium between the extrusion rate and the printing speed. Furthermore, a significant enhancement in geometric quality was evident compared to the empirical setup, particularly in terms of interlayer adhesion, edge resolution, and dimensional stability.

Figure 4. 3D printing using mathematical model parameters.

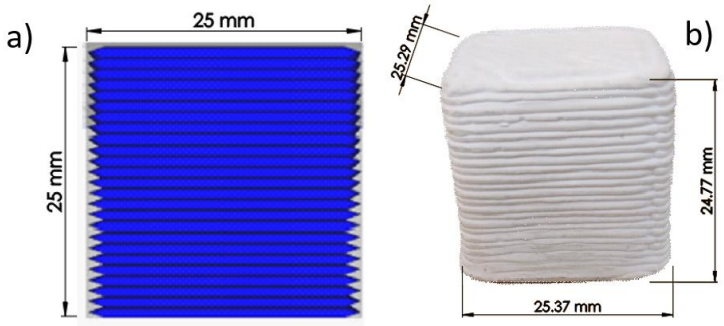

Source: own elaboration.

Figure 4a-b demonstrates a concordance between the computer simulation and the printed part. Notably, Figure 4a exhibits an upward curvature along the *z* axis, a characteristic of the material used in the simulation. This behavior is clearly visible in the 3D printed cube depicted in Figure 4b, thus validating the simulation - printing process.

The experimental measurements obtained as follows: 25.29 mm on the x -axis, 25.37 mm on the y -axis, and 24.77 mm on the z -axis (see Figure 4b). These measurements yield percentage errors of 1.16%, 1.48%, and 0.92% for each axis, respectively. The greatest discrepancy occurred on the z -axis due to filament flattening during nozzle-substrate contact. However, the error obtained is considered minimal and provides a measure of confidence for printing more complex three-dimensional shapes.

In comparison to previously reported work, while numerous studies prioritize dimensional variation associated with drying and sintering, *as- printed errors* are only occasionally reported explicitly. In the study by Ordoñez et al. (2019), the post-processing dimensional change is primarily quantified; however, based on the values presented in their figures, it can be inferred that the Vf-53-Pol-0.8A and Vf-50-Sil-0.8A formulations exhibit the smallest deviations, with approximate errors of 2.43% in diameter and 3.80% in height for the first printed layer, and 1.30% in diameter and height for the second printed layer.

As a final result, a piece with complex geometry was printed to evaluate the stability of the deposition under variations in slope and extended trajectories. Figure 5 shows the side view of the printed specimen, where a structure with adequate uniformity between layers and continuous interfilament cohesion can be observed. The printing time was 52 minutes. The absence of localized collapses and irregular accumulations confirms that the paste maintained its resistance to deformation during stacking, thereby preserving the target shape, even in regions with greater curvature.

Figure 5. 3D printing of a vessel with complex geometry.

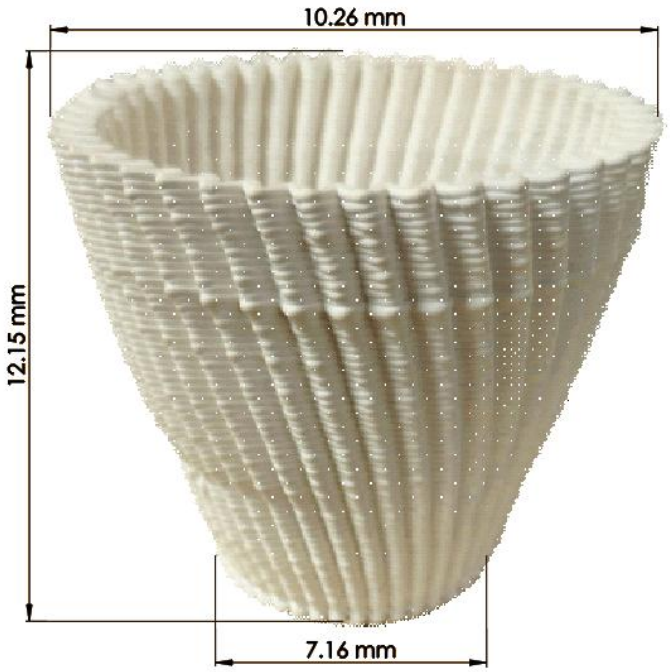

Source: own elaboration.

The container showed impermeable behavior, evidenced by its insolubility and the absence of leakage or dripping during filling tests. This supports the integrity of the deposition and the layer-by-layer densification achieved.

The practical validity of the mathematical model reinforces its applicability as a calibration tool for 3D printing systems employing direct extrusion on ceramic pastes. This approach is applicable to other extrusion systems with a similar design, provided the model's assumptions are maintained, particularly the constancy of the flow and the homogeneity of the material during extrusion.

Discussion

Experimental results show that the relationship between extrusion and printing speeds is a determining factor for geometric stability and print quality. Empirical tuning identified a functional operating window; however, it revealed limitations in terms of dimensional accuracy and structural collapse.

The comparison between the empirical and theoretical fit reveals that the mathematical model provides a more accurate match between the extrusion speed (v_e) and the displacement speed (v_{xy}). Furthermore, the dimensional errors obtained in *the as- printed state* are within a valid

range. However, the study has certain limitations. In particular, the model assumes a constant volumetric flow rate and homogeneous behavior of the ceramic paste, without considering rheological effects, humidity variations, or deformations induced by self-weight in taller geometries. In the work of Buswell et al., it is noted that the apparent density and the presence of voids due to underextrusion depend on the synchronization between the volumetric flow rate, the speed, and the filament thickness. It is also indicated that changes in direction and radii of curvature influence the appearance of underfilled zones.

Although the referenced article mentions that, while it is theoretically possible to compensate for this by adjusting the layer height and flow rate, achieving such compensation with precision and repeatability is difficult in practice. These considerations align with the flow balance calibration strategy implemented in this study. By applying this technique, potential local mismatches between flow rate and velocity, are minimized, particularly when the flow paths are long and curved (Buswell et al., 2018).

Furthermore, in DIW ceramic systems, the paste composition, nozzle diameter, and geometric stability are primarily influenced by the volumetric flow rate. In this context, Ordoñez et al. (2019) quantified the flow rate as a function of nozzle diameter and demonstrated that, without adjusting the extrusion speed and layer pitch, increasing the flow rate results in overextrusion, deterioration of the surface finish, and reduced dimensional stability. Their study showed that altering the nozzle diameter from 1.5 mm to 2.5 mm resulted in less stable parts with lower geometric quality; therefore, they opted to select the smaller diameter nozzle.

Conclusions

This work developed a theoretical - experimental scheme for calibrating a 3D printer for ceramic materials based on direct extrusion. The ceramic paste consists of a Ready-Mix acrylic base, white cement, kaolin, and borax. The theoretical - experimental calibration demonstrated that empirical adjustment allows for the identification of functional operating ranges, while the mathematical model optimizes key printing parameters, achieving an optimal extrusion speed of v_e=22.09 mm/s and a displacement speed of v_{xy}=17.08 mm/s. Consequently, continuous and stable material deposition with good geometric resolution was achieved. The results confirm that mathematical models constitute a robust tool for optimizing DIW-type additive manufacturing processes. Furthermore, a reliable calibration

methodology is established, applicable to different 3D printer models, facilitating the incorporation of new materials, the printing of more complex geometries and its implementation in the biomedical, construction, and high-tech industries.

Future Lines of Research

The modification of the ceramic paste is being considered, involving an experimental study to determine its rheological properties and a visual inspection analysis to determine its geometric quality. The primary outcome of this modification can be incorporated into the mathematical model, expanding its application range and improving its quality in 3D printing. Furthermore, a controlled experimental design is required to systematically establish the ambient temperature and humidity conditions, which influence the drying rate and the appearance of cracks.

Acknowledgments

The first author expresses his gratitude to the Secretariat of Science, Humanities, Technology and Innovation (Secihti), for the support received through the doctoral scholarship with code 2025-DR-006645.

References

Avila-Navarrete, J. J., y Muñoz-Gómez, J. A. (2025). Pasta cerámica de bajo costo para impresión 3D. Revista Ciencia Aplicada, 1(1), 10-22. https://doi.org/10.66482/m15k1012

Bose, S., Akdogan, E. K., Balla, V. K., Ciliveri, S., Colombo, P., Franchin, G., Ku, N., Kushram, P., Niu, F., Pelz, J., Rosenberger, A., Safari, A., Seeley, Z., Trice, R. W., Vargas-Gonzalez, L., Youngblood, J. P., y Bandyopadhyay, A. (2024). 3D printing of ceramics: Advantages, challenges, applications, and perspectives. *Journal of the American Ceramic Society*. *American Ceramic Society*, 107(12), 7879–7920. https://doi.org/10.1111/jace.20043

Alonso Madrid, J., Sotorrío Ortega, G., Gorostiza Carabaño, J., Olsson, N. O. E. y Tenorio Ríos, J. A. (2023). 3D claying: 3D printing and recycling clay. *Crystals*, 13(3), 375. https://doi.org/10.3390/cryst13030375

Buswell, R. A., Leal de Silva, W. R., Jones, S. Z. y Dirrenberger, J. (2018). 3D printing using concrete extrusion: A roadmap for research. *Cement and Concrete Research*, 112, 37–49. https://doi.org/10.1016/j.cemconres.2018.05.006

Carter, C. B. y Norton, M. G. (2013). *Ceramic Materials: Science and Engineering* (2.ª ed.). Springer New York. https://doi.org/10.1007/978-1-4614-3523-5

Chen, H., Guo, L., Zhu, W. y Li, C. (2022). Recent advances in multi-material 3D Printing of functional ceramic devices. *Polymers*, 14(21), 4635. https://doi.org/10.3390/polym14214635

Chen, Y., He, S., Zhang, Y., Wan, Z., Çopuroğlu, O. y Schlangen, E. (2021). 3D printing of calcined clay-limestone-based cementitious materials. *Cement and Concrete Research*, 149, 106553. https://doi.org/10.1016/j.cemconres.2021.106553

Conner, B. P., Manogharan, G. P., Martof, A. N., Rodomsky, L. M., Rodomsky, C. M., Jordan, D. C. y Limperos, J. W. (2014). Making sense of 3-D printing: Creating a map of additive manufacturing products and services. *Additive Manufacturing*, 1, 64–76. https://doi.org/10.1016/j.addma.2014.08.005

Diegel, O., Withell, A., de Beer, D., Potgieter, J. y Noble, F. (2012). Low-cost 3D printing of controlled porosity ceramic parts. *International Journal of Automation Technology*, 6(5), 618–626. https://doi.org/10.20965/ijat.2012.p0618

Feng, C., Zhang, M., y Bhandari, B. (2019). Materials Properties of Printable Edible Inks and Printing Parameters Optimization during 3D Printing: a review. *Critical Reviews in Food Science and Nutrition*, 59(19), 3074–3081. https://doi.org/10.1080/10408398.2018.1481823

Ford, S. y Despeisse, M. (2016). Additive manufacturing and sustainability: an exploratory study of the advantages and challenges. *Journal of Cleaner Production*, 137, 1573–1587. https://doi.org/10.1016/j.jclepro.2016.04.150

Gibson, I., Rosen, D., y Stucker, B. (2015). *Additive manufacturing technologies: 3D printing, rapid prototyping, and direct digital manufacturing* (2.ª ed.). Springer. https://doi.org/10.1007/978-1-4939-2113-3

Hu, F., Mikolajczyk, T., Pimenov, D. y Gupta, M. (2021). Extrusion-Based 3D Printing of Ceramic Pastes: Mathematical Modeling and In Situ Shaping Retention Approach. *Materials*, 14(5), 1137. https://doi.org/10.3390/ma14051137

Lewis, J. A. (2006). Direct Ink Writing of 3D Functional Materials. *Advanced Functional Materials*, 16(17), 2193–2204. https://doi.org/10.1002/adfm.200600434

Lewis, J. A. y Gratson, G. M. (2004). Direct writing in three dimensions. *Materials Today*, 7(7), 32–39. https://doi.org/10.1016/S1369-7021(04)00344-X

Lin, T., Zhao, Z., Wang, T. y Pan, Y.-T. (2023). Three-Dimensional Printing of Large Ceramic Products and Process Simulation. *Materials*, 16(10), 3815. https://doi.org/10.3390/ma16103815

Ngo, T. D., Kashani, A., Imbalzano, G., Nguyen, K. T. Q. y Hui, D. (2018). Additive manufacturing (3D printing): A review of materials, methods, applications and challenges. *Composites Part B: Engineering*, 143, 172–196. https://doi.org/10.1016/j.compositesb.2018.02.012

Ordoñez, E., Gallego, J. M. y Colorado, H. A. (2019). 3D printing via the direct ink writing technique of ceramic pastes from typical formulations used in traditional ceramics industry. *Applied Clay Science*, 182, 105285. https://doi.org/10.1016/j.clay.2019.105285

Romanczuk-Ruszuk, E., Sztorch, B., Pakuła, D., Gabriel, E., Nowak, K. y Przekop, R. E. (2023). 3D Printing Ceramics-Materials for Direct Extrusion Process. *Ceramics*, 6(1), 364–385. https://doi.org/10.3390/ceramics6010022

Somiya, S. (2013). *Handbook of Advanced Ceramics: Materials, Applications, Processing, and Properties* (2.ª ed.). Academic Press. https://doi.org/10.1016/C2010-0-66261-4

Tagliaferri, S., Panagiotopoulos, A. y Mattevi, C. (2021). Direct ink writing of energy materials. *Materials Advances*, 2(2), 540–563. https://doi.org/10.1039/d0ma00753f

Yan, Q., Dong, H., Su, J., Han, J., Song, B., Wei, Q. y Shi, Y. (2018). A Review of 3D Printing Technology for Medical Applications. *Engineering*, 4(5), 729–742. https://doi.org/10.1016/j.eng.2018.07.021

Yousaf, A., Al Rashid, A. y Koç, M. (2024). Parameter tuning for sustainable 3D Printing (3DP) of clay structures. *Journal of Engineering Research (Kuwait)*, 11(3), 1826-1842. https://doi.org/10.1016/j.jer.2024.05.027

Zaborovskii, N., Masevnin, S., Smekalenkov, O., Murakhovsky, V. y Ptashnikov, D. (2025). Patient-specific 3D-Printed PEEK implants for spinal tumor surgery. *Journal of Orthopaedics*, 62, 99–105. https://doi.org/10.1016/j.jor.2024.10.024

Contribution Role	Author(s)
Conceptualization	José Antonio Muñoz Gómez
Methodology	Juan José Avila Navarrete Omar Aguilar Loreto (same)
Software	Not Applicable
Validation	Juan José Avila Navarrete
Formal Analysis	Omar Aguilar Loreto Abimael Jiménez Pérez
Investigation	Juan José Avila Navarrete
Resources	Juan José Avila Navarrete (principal) José Antonio Muñoz Gómez (supports)
Data curation	Not Applicable
Writing - Preparing the original draft	José Antonio Muñoz Gómez Juan José Avila Navarrete Omar Aguilar Loreto (same)
Writing - Reviewing and Editing	José Antonio Muñoz Gómez (principal) Omar Aguilar Loreto (supports) Abimael Jiménez Pérez (supports)
Display	Abimael Jiménez Pérez Omar Aguilar Loreto (same)
Supervision	José Antonio Muñoz Gómez
Project Management	José Antonio Muñoz Gómez (principal) Abimael Jiménez Pérez (supports)
Acquisition of funds	Not Applicable